Supporting Information

Tordella et al. 10.1073/pnas.1309362110

SI Materials and Methods

Mouse Colonies. *ASPP2* Δexon3 mutant mice were generated as described previously (1) and backcrossed to a BALB/c background for nine generations. *ASPP2* Δexon3 mutant mice were genotyped as described in Vives et al. (1), using the following primers: 5′-CTCCACCCCAGGAAATTACA-3′ (intron 3), 5′-CGGTTTGGAAGTCAAAGGAA-3′ (exon 3), and 5′-GGA-CCGCTATCAGGACATA-3′ (neomycin resistance gene). *p53* heterozygous mice (on a BALB/c background) were generated by G.L.'s group. *p53* and *ASPP2* single heterozygous mice were crossed together to generate double heterozygotes. The latter were intercrossed to generate compound genotypes. *p53* KO mice were genotyped using the following primers: 5′-CCC-GAGTATCTGGAAGACAG-3′ (exon 6), 5′-ATAGGTCGGC-GGTTCAT-3′ (exon 7), and 5′-GGACCGCTATCAGGACA-TA-3′ (neomycin resistance gene). *p63* heterozygous mice (on a BALB/c background) were generated by F.D.M.'s group. *p63* and *ASPP2* single heterozygous mice were crossed together to generate double heterozygotes. The latter were intercrossed to generate compound genotypes. *p63* KO mice were genotyped using the following primers: 5′-TTCTCAGATGGTACC-GCTCC-3′ (exon 3), 5′- GGTGCTTTGAGGCCCGGATC-3′ (exon 4), and 5′- TACCCGCTTCCATTGCTCAG-3′ (neomycin resistance gene).

Tumor Processing and Analysis. Mice that developed visible tumors or showed signs of ill health were killed and subjected to necropsy with careful examination for tumors. Tumors and samples from other organs were fixed in 10% (wt/vol) buffered formalin and processed for histology. Sections 4 μm thick were stained with H&E. Tumor characterization at the morphological level (macroscopic and H&E), before immunohistochemistry, was conducted by V.S., R.D.G., and F.F.

Tissue Section Staining. Rehydrated paraffin-embedded sections were microwaved in 10 mM sodium citrate buffer, pH 6, incubated in 3% (vol/vol) hydrogen peroxide in methanol, washed in PBS solution, blocked with 5% (vol/vol) goat serum in PBS solution for 1 h at room temperature (RT), and then incubated overnight (O/N) at 4 °C with the primary antibody diluted in blocking solution. Subsequently, sections were incubated with biotinylated or Alexa Fluor (1:400; Molecular Probes) secondary antibody for 30 min at RT and then washed in PBS solution. Sections incubated with fluorescent secondary antibodies were mounted and analyzed by confocal microscopy (Zeiss), whereas sections incubated with biotinylated secondary antibodies were first treated with the peroxide substrate solution diaminobenzidine (Vector), followed by dehydration, mounting, and analysis by phase-contrast microscopy. Human skin and cervical tissue samples (tumor and normal) were provided by R.D.G. Human head and neck squamous cell carcinoma (SCC) tissue samples were provided by M.T. Human head and neck tissue array was provided by H.M., G.F.H., and M.R.

Tissue Microarray Analysis. ASPP2 expression was scored based on the intensity of staining (0, none; 1, weak; 2, moderate; 3, strong) and the proportion of cells exhibiting staining (0–100% in 5–10% increments). The overall expression is a product of these two scores [expression = intensity × proportion (0–300)]. Statistical analysis was undertaken using SPSS Statistics software. Results were analyzed by the Kruskal–Wallis test (i.e., *H* test) with Mann–Whitney tests (i.e., *U* test) used for post hoc procedures, and the effect size is denoted by $r = z/\sqrt{n}$ (>0.3 represents medium effect, >0.5 represents large effect). A Bonferroni correction was applied so all effects are reported at a 0.0167 (i.e., 0.05/3) level of significance.

Cell Culture and Generation of Primary Cells. Mouse embryonic fibroblasts (MEFs) and mouse primary keratinocytes (PKs) were prepared and cultured as described previously (2) from $ASPP2^{\Delta exon3/+}$ mice. Undifferentiated mouse PKs and HaCat cells were differentiated by the addition of $CaCl_2$ in the medium to a final concentration of 1.2 mM. SCC cell lines (3) were cultured in DMEM supplemented with L-glutamine, penicillin/streptomycin, 10% (vol/vol) FCS, and nonessential amino acids (Sigma-MEM solution).

Cell Transfection and Electroporation. FuGene6 (Promega) transfection and electroporation (Amaxa) were used according to the manufacturers' protocols.

siRNAs. siRNA oligos against Notch1, NF-κB/p65, ASPP2, and RISC-Free siRNA were purchased from Dharmacon. Cells were transfected with the indicated siRNA oligos at a final concentration of 35 nM using Dharmafect 1 reagent (Dharmacon) according to the manufacturer's instructions.

Immunoblotting and Immunoprecipitation. Cell lysates of the 34 SCC cell lines panel were generated as previously described (3). For all other immunoblots cells were lysed in buffer, containing 10 mM Tris·Cl (pH 8.0), 140 mM NaCl, 1 mM EDTA, 0.5 mM EGTA, 1% Triton X-100, 0.1% sodium deoxycholate, 0.1% SDS, and Complete Protease Inhibitor Mixture (Roche). Protein concentration was estimated using Bradford assay. Protein extracts were loaded onto SDS-polyacrylamide gels. Gels were transferred onto nitrocellulose membranes (Protran) and the resulting blots incubated first with primary antibody overnight at 4 °C, then with the appropriate secondary HRP-conjugated antibody (Dako). The results were visualized by enhanced chemiluminescence detection (Amersham Biosciences) using X-ray film (Fujifilm). For immunoprecipitation, cell lysates were produced in the same manner. To reduce nonspecific binding in the immunoprecipitation assay, cell lysates were precleared using Protein G Sepharose 4 Fast Flow beads (GE Healthcare Bio-Sciences). Protein concentration was determined as before, and 0.5 to 1 mg of extracts were incubated with antibody prebound to protein G beads overnight. Immunoblots were carried out as described earlier.

Real-Time Quantitative PCR. Real-time quantitative PCR (RT-qPCR) was performed with the 7500 real-time PCR system (Applied Biosystems) using the QuantiTect SYBR Green PCR kit (Qiagen). Each reaction was performed in triplicate using 1 μL of cDNA in a final volume of 25 μL. The expression level of each target gene was analyzed based on the ΔΔCt method, with *GAPDH* as an internal control. The following thermal cycle was used for all samples: 15 min at 95 °C; 45 cycles of 15 s at 94 °C, 30-s primer-specific annealing temperatures, 1 min at 72 °C. For each experiment, the threshold was set to cross a point at which real-time PCR amplification was linear. Previously published primers were used for all genes analyzed (Table S3 provides sequences).

Immunofluorescence Staining. Cells were washed with PBS solution and fixed in 4% (wt/vol) paraformaldehyde (Sigma-Aldrich). Permeabilization was performed with 0.1% Triton X-100

solution on ice for 4 min. Blocking solution composed of 0.2% fish gelatin (Sigma-Aldrich) was applied for 30 min, following incubation with the appropriate diluted primary antibodies for 1 h at RT. Then, cells were incubated with Alexa Fluorochrome secondary antibody (1:400; Molecular Probes) and TO-PRO (Invitrogen) or DAPI (Roche) to stain nucleic acids, for 1 h at RT. Finally, cells were mounted with Mowiol onto glass slides and samples were analyzed by confocal microscopy.

Statistical Analysis. Comparisons between the genotype frequencies were performed by using the χ^2 test. The log-rank (Mantel–Cox) test was used to determine the statistical significance of differences in tumor-free survival studies. The Wilcoxon rank-sum test was used in Fig. S4*I*, whereas the *t* test was used for all other measurements. Differences were considered significant at a value of $P \leq 0.05$. ImageJ software was used to quantify gel bands from immunoblots.

1. Vives V, et al. (2006) ASPP2 is a haploinsufficient tumor suppressor that cooperates with p53 to suppress tumor growth. *Genes Dev* 20(10):1262–1267.
2. Notari M, et al. (2011) Inhibitor of apoptosis-stimulating protein of p53 (iASPP) prevents senescence and is required for epithelial stratification. *Proc Natl Acad Sci USA* 108(40):16645–16650.
3. Wu Z, et al. (2011) Quantitative chemical proteomics reveals new potential drug targets in head and neck cancer. *Mol Cell Proteomics* 10(12):M111.011635.

A

B

C

D

E

Fig. S1. (*A*) Double immunofluorescence (IF) staining of mouse epidermis using anti-ASPP2 and anti-p63 antibodies. (Scale bar: 20 μm.) (*B*) H&E, ASPP2, and p63 immunostain (diaminobenzidine) of consecutive sections of human cervical epithelium. (Scale bar: 50 μm.) (*C*) ASPP2 and keratin-4 (K4) and ASPP2 and keratin-14 (K14) double IF of sections of mouse esophageal epithelium. (Scale bar: 30 μm.) (*D*) ASPP2 immunostain of sections of human esophageal epithelium. (Scale bar: 50 μm.) Squares in *C* and *D* show highly magnified views of the regions where ASPP2 is expressed. White line marks the basal membrane. (*E*) ASPP2 and p63 immunostain in mouse primary esophageal keratinocytes before and after incubation with Ca^{2+} for 3 d, as indicated. (Scale bar: 10 μm.) Nuclei were counterstained with DAPI (*C* and *E*) or TO-PRO (*D*).

Fig. S2. (Continued)

Fig. S2. (*A*) Birth rate of pups after weaning (P30, postnatal day 30) for each of the three possible genotypes generated by the intercross between $ASPP2^{\Delta exon3/+}$ mice is shown ($n = 236$), comparing the expected Mendelian frequency (in white) with the observed frequency (in black). (*B*) Overall survival study of $ASPP2^{+/+}$, $ASPP2^{\Delta exon3/+}$, and $ASPP2^{\Delta exon3/\Delta exon3}$ mice over a period of 80 wk [$^{*}P = 0.012$ and $^{***}P < 0.0001$, log-rank (Mantel–Cox) test]. (*C*) Tumor-free survival of male and female $ASPP2^{\Delta exon3/+}$ mice from the study in Fig. 2*A*. No significant differences were observed between the sexes by log-rank (Mantel–Cox) test ($P = 0.3$). (*D*) Graph showing the frequency of localization for tumors found in $ASPP2^{\Delta exon3/+}$ mice. Tumors were found in the neck (28%), abdomen (29%), and flank (25%) regions with similar frequency, and with a lower frequency of onset in the chest (15%) and back (4%). (*E*) Example of an $ASPP2^{\Delta exon3/+}$ mouse affected by a spontaneous tumor. Empty arrowhead indicates site of tumor. Size of tumor harvested is shown at lower left (approximately 1 cm long). (*F*) Example of H&E-stained section of SCC (*i*, barrel-shaped masses of tumor cells; *i*′, higher magnification of tumor cells; *n*, necrotic region). (*G*–*I*) SCC H&E-stained section showing regions of tumor invasion into the stroma (*G*), and an example of blood vessel invasion by tumor cells (*H*) and high mitotic index (*I*). (Scale bars: *F*–*I*, 50 μm.) (*J* and *K*) Double IF for different cell markers performed in four consecutive sections of the same tumor area from an $ASPP2^{\Delta exon3/+}$ mouse. White squares define areas within the tumor sections presented at higher magnification (*Right*). (*J*) Coexpression of K14–K1 and K14–p63 in the tumor cell population. (*K*) Tumor cells marked by K14 staining are not positive for vimentin (expressed in the stromal compartment) or keratin-18 (K18; expressed in the ductal epithelium). (Scale bars: 80 μm.) (*L*) Immunostains for total-p63 (4A4 antibody), TAp63 (Poly6189 antibody), and ΔNp63 (Poly6190 antibody) in consecutive sections of the same tumor area from an $ASPP2^{\Delta exon3/+}$ mouse. Nuclei were counterstained with DAPI. (Scale bar: 20 μm.) (*M*) Immunoblot showing the specificity of anti-p63 antibodies for total p63 (4A4), TAp63 (Poly6189), and ΔNp63 (Poly6190). H1299 cell lysates transfected with empty vector (–), TAp63α, or ΔNp63 expression vectors were labeled as indicated. β-Tubulin was used as a loading control. (*N*) mRNA from tumors of $ASPP2^{\Delta exon3/+}$ mice and normal skin controls from the same mice ($n = 3$) were analyzed by RT-qPCR to assess the expression of the indicated genes. *TAp63* and *ΔNp63* were significantly upregulated in tumors ($^{*}P = 0.035$ and $^{**}P = 0.0024$). Data are expressed in arbitrary units, using *GAPDH* for internal normalization. Bar graph values are the mean ± SD of experiments performed using three different pairs of tumor/normal tissue.

Fig. S3. (*A*) Genotype distributions of 211 pups born from the intercross between $ASPP2^{\Delta exon3/+}$ and $p53^{+/-}$ mice. The Mendelian segregation frequency (expected) and the observed frequency (observed) are shown. The absence of p53 negatively affects the number of *ASPP2* mutant mice born, whereas double heterozygous mice develop normally and compensate for the absence of other genotypes (*$P = 0.02$ and ***$P < 0.002$, χ^2 test). (*B*) Tumor-free survival study in *ASPP2/p53* compound mice (cohort in *A*) over a period of 100 wk [*$P = 0.02$, log-rank (Mantel–Cox) test]. (*C*) Graph showing incidence of different tumor types with indicated genotypes. (*D–F*) Tumor-free survival of indicated *ASPP2/p53* compound mice over a period of 100 wk. *p53* and *ASPP2* status are indicated [*$P < 0.04$ and ***$P < 0.0001$, log-rank (Mantel–Cox) test]. (*G* and *H*) H&E staining of tumor sections showing examples of tumor types found in the *ASPP2/p53* (*G*) and *ASPP2/p63* study (*H*). A higher magnification view is presented at lower left in each panel. (Scale bars: 100 μm.)

Fig. S4. (Continued)

Fig. S4. (*A*) Quantification of ASPP2- and p63-expressing cells within SCCs of $ASPP2^{\Delta exon3/+}$ mice. Bar graph values are the mean ± SD from quantification of immunostains of three different tumors. (*B*) Agarose gel analysis of ASPP2 alleles using genomic DNA from tumors and matching tails of five different $ASPP2^{\Delta exon3/+}$ mice. Control DNA from another $ASPP2^{\Delta exon3/+}$ mouse was used as comparison (+). The presence of the two bands indicates *ASPP2* heterozygosity, as indicated. (*C*) Double IF of ASPP2 and p63 in a section of human cutaneous SCC. Regions expressing ASPP2 are negative for p63 expression (white arrows). The white box marks a region viewed at higher magnification. TO-PRO was used to visualize nuclei. (Scale bar: 20 μm.) (*D*) Analysis of the expression levels of *ΔNp63* and *TAp63* mRNA in MEFs and PKs after 24 and 34 PCR cycles. Analysis of *GAPDH* mRNA was used as a positive control for the PCR. After 34 PCR cycles, the expression of *ΔNp63* was approximately 14-fold higher than that of *TAp63*. (*E*) RT-qPCR analysis of expression levels of *ΔNp63* and *TAp63* mRNA (actual detection) in mouse PKs (whole epidermis). The difference in *ΔNp63* mRNA in *ASPP2* WT vs. *ASPP2* Δexon3 keratinocytes was approximately threefold (*$P = 0.034$; *n* indicates the number of littermate-paired PKs used). *GAPDH* expression was used as an internal control. Bar graph values are the mean ± SD from three different experiments. (*F*) RT-qPCR analysis of the expression levels of *ΔNp63* and *TAp63* mRNA in MEFs derived from $ASPP2^{+/+}$ (WT) and $ASPP2^{\Delta exon3/\Delta exon3}$ (Δexon3) BALB/c mice. The difference in *ΔNp63* mRNA in WT vs. Δexon3 MEFs was approximately sixfold (*$P = 0.016$; *n* indicates number of littermate-paired MEFs used in the analysis). The expression of *GAPDH* was used as an internal control. Bar graph values are the mean ± SD from three different experiments. (*G*) Immunoblot showing p63 expression levels in MEFs, with actin as a loading control. (*H*) Immunoblot showing the expression levels of ASPP2, p63, and iASPP in a panel of 34 SCC cell lines as indicated. Samples highlighted in frames are examples of cell lines with high p63 expression (green), corresponding to low ASPP2 expression (red). The cell lines marked by both frames were given an identical number at the bottom of the frames. (*I*) Box plot showing mean p63 and ASPP2 expression in SCC cell lines (**$P = 0.0009$, Wilcoxon rank-sum test). (*J*) Quantification of ASPP2 and p63 protein expression levels based on the Western blot shown in Fig. S4*H*. The expression bands from the gel were quantified by using ImageJ software. ASPP2 and p63 expression values were normalized on iASPP expression, as it appeared to be fairly constant in all 34 lines analyzed. Arrowheads indicate three different groups of cell lines,

Legend continued on following page

divided according to their p63:ASPP2 expression ratio (yellow, 1:1; red, 2:1 or higher; blue, 1:2 or lower). (*K*) Scatterplot showing the distribution of 34 SCC cell lines according to their ratio of p63:ASPP2 expression: 1:1 (yellow dots), 2:1 or higher (red dots), and 1:2 or lower (blue dots). (*L*) Double IF of HSC3 cells to detect transfected ASPP2-V5 and endogenous p63, using anti-V5 and anti-p63 antibodies. TO-PRO was used to visualize nuclei. Cells expressing ASPP2-V5 and low levels of p63 are labeled with white arrows. The graph shows the percentage of $V5^{+}/p63^{-}$ cells in the ASPP2-V5 transfected sample compared with the $p63^{-}$ cells in the empty vector-transfected samples (values are the mean ± SD from three different experiments; $***P < 0.0001$). (Scale bar: 10 μm.) (*M*) RT-qPCR expression analysis of *ΔNp63* mRNA in UPCI-SCC-040 cells upon transfection with a *GFP*- or *ASPP2*-expression construct. In ASPP2 transfected cells, *ΔNp63* mRNA is down-regulated by approximately 40% compared with GFP transfected cells ($*P = 0.031$). *GAPDH* was used as an internal control. Bar graph values are the mean ± SD from quantification of three different experiments. (*N* and *O*) Immunoblot analysis of p63 and iASPP-V5 (blot V5) protein levels upon exogenous expression of iASPP-V5 or empty vector (*N*) or p63 and ASPP2 protein levels upon ASPP2 siRNA or CTR siRNA (*O*), in HaCat cells cultured in high Ca^{2+} for 5 d, with β-tubulin as a loading control. (*Right*) RT-qPCR expression analysis of *TAp63*, *ΔNp63*, *sp100* (used as unrelated control gene), and *iASPP* or *ASPP2* mRNA for the same samples, as indicated ($***P < 0.0001$). In all RT-qPCR experiments, *GAPDH* was used as an internal control. Bar graph values are the mean ± SD from quantification of three different experiments.

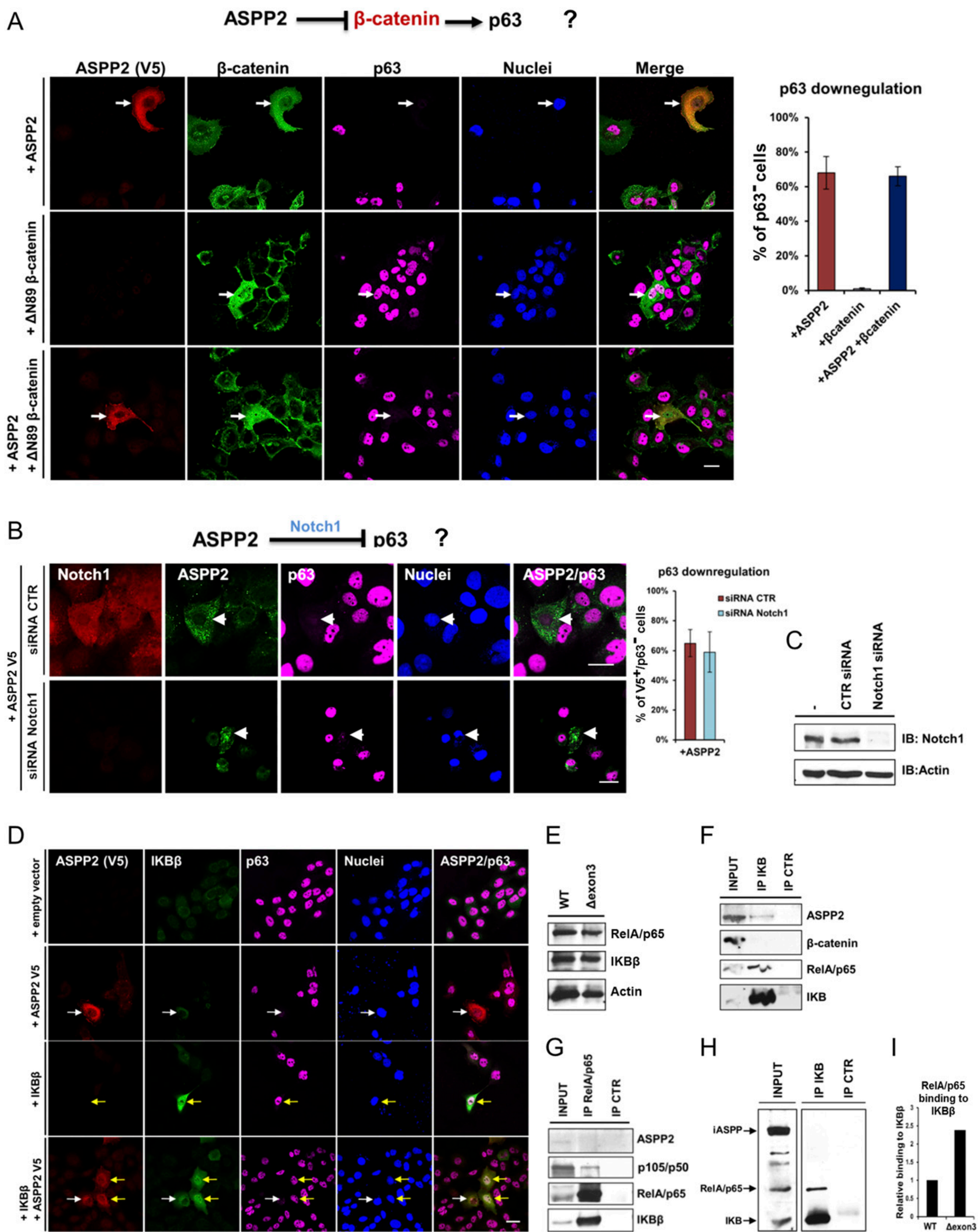

Fig. S5. (*A*) Triple IF staining of UPCI-SCC-040 cells to detect transfected ASPP2-V5 (red) and/or ΔN89 β-catenin (green) with endogenous p63 (magenta), using anti-V5 (goat), anti–β-catenin (rabbit), and anti-p63 (mouse) antibodies. Transfected cells are labeled by white arrows. The graph represents the percentage of ASPP2-V5$^+$ and/or β-catenin$^+$ cells that have down-regulated p63 compared with the empty vector-transfected cells. (*B*) Triple IF staining of UPCI-SCC-040 cells using anti-Notch1 (goat), anti-V5 (rabbit), and anti-p63 (mouse) antibodies. Cells were previously treated with Notch1 siRNA or control siRNA (CTR) and then transfected with an ASPP2-V5 expression vector. ASPP2-V5–transfected cells are labeled by white arrows. The graph represents the percentage of ASPP2-V5$^+$/p63$^-$ cells in cells treated with siRNA-Notch1 vs. control siRNA. (*C*) Immunoblot analysis of Notch1 protein levels in cells transfected with Notch1 siRNA, compared with

Legend continued on following page

control siRNA-transfected cells and untransfected cells (–). Actin was used as a loading control. (*D*) Triple IF staining of UPCI-SCC-040 cells to detect transfected ASPP2-V5 (red) and/or IκBβ (green) with endogenous p63 (magenta), using anti-V5 (goat), anti-IκBβ (rabbit), and anti-p63 (mouse) antibodies. Cells expressing transfected ASPP2-V5 and low (white arrow) or high levels of transfected IκBβ (yellow arrows) are labeled. (*E*) Immunoblot analysis of RelA/p65 and IκBβ protein levels in *ASPP2*$^{+/+}$ (WT) and *ASPP2*$^{\Delta exon3/\Delta exon3}$ (Δexon3) MEFs. Actin was used as a loading control. (*F*) Lysates from *ASPP2* WT MEFs immunoprecipitated by using a mouse monoclonal anti-IκBβ (IP IκBβ) or mouse IgG (IP CTR) antibody and immunoblotted using rabbit anti-ASPP2, β-catenin, RelA/p65, and IκBβ antibodies. (*G*) Lysates from *ASPP2*$^{+/+}$ MEFs were immunoprecipitated by using a rabbit polyclonal anti-RelA/p65 (IP RelA/p65) or rabbit IgG (IP CTR) antibody, then immunoblotted using mouse anti-ASPP2, p105/p50, RelA/p65, and IκBβ antibodies. IκBβ and p105/p50, but not ASPP2, were found to be coimmunoprecipitated with RelA/p65. (*H*) Lysates from *ASPP2* WT MEFs immunoprecipitated using a mouse monoclonal anti-IκBβ (IP IκBβ) or mouse IgG (IP CTR) antibody and immunoblotted using rabbit anti-iASPP, RelA/p65, and IκBβ antibodies. (*I*) ImageJ quantification of the immunoblot in Fig. 5*E*, comparing the amounts of RelA/p65 immunoprecipitated with IκBβ in *ASPP2* WT vs. Δexon3 MEFs. RelA/p65 levels were normalized by the amount of IκBβ immunoprecipitated in each sample before comparison. In *A*, *B*, and *D*, DAPI was used to visualize the nuclei. (Scale bars: 10 μm.) Bar graph values are the mean ± SD from three different experiments.

Fig. S6. ASPP2 expression is decreased during tumor progression in a large cohort of human SCC samples. (*A*) (*Top*) Example of human biopsies of non-transformed squamous epithelia ($n = 12$). Human SCC of head and neck tissue array, comprising various grades of tumor progression for a total of 318 carcinoma cores, analyzed by immunostaining using an anti-ASPP2 antibody. Regions positive for ASPP2 expression are shown at higher magnification. (Scale bar: 50 μm.) (*B*) Quantification of the tissue array immunostain indicating ASPP2's expression in the different tumor types analyzed ($*P < 0.01$). (*C*) Graph shows ASPP2 expression among p63-negative and p63-positive groups of human primary HNSCCs ($n = 73$). The difference of ASPP2 expression levels between p63-negative and p63-positive HNSCCs is measured by Mann–Whitney test ($*P = 0.042$).

Table S1. Primary antibodies

Antigen	Name	Source	Applications
Actin	C-2	Santa Cruz	WB
ASPP2	S-80	Rabbit polyclonal	IHC
ASPP2	S-32	Rabbit polyclonal	IHC, WB
ASPP2	DX54.10	Mouse monoclonal	IHC, WB
ASPP2	LX50.13	Mouse monoclonal	WB
Envoplakin	M-20	Santa Cruz	WB
iASPP	LX49.3	Mouse monoclonal	IHC, WB
IκBβ	C-20, D-3	Santa Cruz	ICC, WB
Keratin-1	AE1	Abcam	IHC
Keratin-4	5H5	Sigma	IHC
Keratin-14	PRB-155P-100	Covance	IHC
Keratin-18	C-04	Abcam	IHC
Loricrin	PRB-145P	Covance	WB
Notch1	C-20	Santa Cruz	WB, ICC
p63 (total)	4A4	Santa Cruz	IHC, ICC, WB
p63 (total)	—	Abcam	IHC, ICC
p63 (TA isoform)	Poly6189	BioLegend	IHC, WB
p63 (ΔN isoform)	Poly6190	BioLegend	IHC, WB
P105/p50	E381	Abcam	WB
V5-tag	SV5-Pk1	Serotec	ICC
V5-tag	—	Abcam	ICC
Vimentin	RV202	Abcam	IHC
β-Catenin	6B3	Cell Signaling	WB
β-Tubulin	TUB 2.1	Abcam	WB

ICC, immunocytochemistry; IHC, immunohistochemistry; WB, Western blot.

Table S2. Plasmids

Name	Vector	Information	Tag	Source
ASPP2	pcDNA3.1	Human ASPP2	V5, His	S. Llanos UCL, London, UK
iASPP	pcDNA3.1	Human iASPP	V5, His	S. Llanos UCL, London, UK
IκBβ	pcDNA3	Human IκBβ	—	N. Rice NCI-FCRDC, Frederick, MD
Control plasmid	pcDNA3.1	Empty vector	V5, His	Invitrogen
GFP	pEGFP-C1	GFP	—	Clontech
ΔN89 β-catenin	pCAN	Human active β-catenin	—	P. Polakis Genentech Inc., San Francisco, CA

Table S3. Primers for RT-qPCR

Name	Sequence (5′-3′)
mGAPDH F	TGTCAGCAATGCATCCTGCA
mGAPDH R	TGTATGCAGGGATGATGTTC
mΔNp63 F	ATGTTGTACCTGGAAAACAATG
mΔNp63 R	GATGGAGAGAGGGCATCAAA
mTAp63 F	AGACAAGCGAGTTCCTCAGC
mTAp63 R	TGCGGATACAATCCATGCTA
hGAPDH F	AATCCCATCACCATCTTCCA
hGAPDH R	TGGACTCCACGACGTACTCA
hΔNp63 F	CAGACTCAATTTAGTGAG
hΔNp63 R	AGCTCATGGTTGGGGCAC
hTAp63 F	ATGTCCCAGAGCACACAG
hTAp63 R	AGCTCATGGTTGGGGCAC
hSP100 F	TCCATGACAAATTGCCTCTCC
hSP100 R	GAGATGGGGAACCCGAAGG

Primers in the table were purchased from Eurofins. Primers for human ASPP2 and human iASPP were purchased from Qiagen (sequences available from Qiagen). F, forward; R, reverse.